Optical transitions of the silicon vacancy in 6*H*-SiC studied by positron annihilation spectroscopy

S. Arpiainen, K. Saarinen, and P. Hautojärvi
Laboratory of Physics, Helsinki University of Technology, 02015 HUT, Finland

L. Henry, M.-F. Barthe, and C. Corbel
Centre d'Etudes et de Recherches par Irradiation, Centre National de la Recherche Scientifique, 3 rue de la Férollerie, Orléans, France
(Received 21 December 2001; published 19 August 2002)

Positron annihilation spectroscopy has been applied to identify Si and C vacancies as irradiation-induced defects in 6*H*-SiC. Si vacancies are shown to have ionization levels at $E_C-0.6$ eV and $E_C-1.1$ eV below the conduction-band edge E_C by detecting changes of positron trapping under monochromatic illumination. These levels are attributed to $(2-/1-)$ and $(1-/0)$ ionizations of the isolated Si vacancy. In as-grown *n*-type 6*H*-SiC, a native defect complex involving V_{Si} is shown to have an ionization level slightly closer to conduction band at roughly $E_C-0.3$ eV. These results are used further to present microscopic interpretations to effects seen in optical-absorption spectra and to electrical levels observed previously by deep-level transient spectroscopy.

DOI: 10.1103/PhysRevB.66.075206 PACS number(s): 71.55.Cn, 73.20.Hb, 61.72.Ji, 78.70.Bj

I. INTRODUCTION

Silicon carbide is a promising semiconductor material for high-power and high-frequency electronics and for high-temperature applications. It recently gained increasing attention due to major progress in the growth techniques, but it remains a difficult material to fabricate. Earlier studies clearly showed that growth at temperatures far above 1000 °C induces defects which inevitably survive to lower temperatures.[1] This results in a significant defect concentration in the as-grown material, and even more defects are introduced in processing techniques such as ion implantation. The defect ionization levels in the energy gap influence electrical properties such as the carrier concentration, lifetime and mobility. To be able to control these effects, it is necessary to identify the defects and to analyze their electron level structures. Theoretical calculations of defect properties have been carried out for different polytypes of SiC,[2–5] but more experimental results are obviously needed. The methods able to resolve the atomic structure of defects would be especially helpful for understanding the origin of various signals seen in conventional electrical and optical measurements. This goal has been partially reached by applying techniques based on electron paramagnetic resonance (EPR) and its optical detection (ODMR).[6–12]

Positron annihilation spectroscopy (PAS) provides efficient means to investigate the atomic structure and charge states of the defects.[13,14] Positrons are trapped by neutral and negatively charged vacancies and localize on the site of the missing ion core. As the positron lifetime is inversely proportional to the overlap of positron and electron densities at the annihilation site, the lifetime τ_v at the vacancy increases with the open volume. The positron lifetime is thus sensitive to the size of the open volume of the defect. In SiC this parameter alone is sufficient to distinguish between monovacancies in the two sublattices because the open volume of the Si vacancy is much larger than that of the C vacancy. The defect identification, however, can be further confirmed by the momentum distribution of annihilating electrons, measured as the Doppler broadening of the 511-keV annihilation line. In addition to vacancies, negatively charged defects with no open volume can also be studied by PAS, since they trap positrons to shallow hydrogenic states. Their effect can only be detected as reduced trapping into vacancies at low temperatures, where positrons do not have enough thermal energy to escape the hydrogenic states.

In silicon carbide, positron annihilation spectroscopy has been used to study native vacancy defects in bulk crystals[15] as well as those formed in electron or proton irradiation[16–22] or ion implantation.[23–25] The positron lifetimes of about 190–230 ps have been attributed to vacancy in the Si sublattice,[16–20,26] and the existing Doppler broadening results[20,27] seem to support this identification. A lifetime of 150–180 ps has also been reported and attributed possibly to the C vacancy.[16,27] Positron lifetime has been further shown to be sensitive to illumination at low temperatures.[28] This is most interesting, because positron spectroscopy under photoexcitation can yield detailed information on the optical processes related to vacancy defects, as indicated by previous results in GaAs and Si.[29–31]

In this work we study optical processes of vacancies both in as-grown 6*H*-SiC and in material irradiated with electrons or protons, by varying both the irradiation energy and fluence. We apply both positron lifetime and two-detector Doppler broadening spectroscopies in order to identify and differentiate between vacancy defects in Si and C sublattices (Sec. III). Experiments under monochromatic illuminations at low temperatures reveal four optical transitions where two ionization levels of the Si vacancy are involved (Sec. IV). We determine the positions of these ionization levels both in as-grown and irradiated material and relate them to absorption edges in optical spectra (Sec. V). We further connect our results with those obtained earlier using electrical techniques, EPR or ODMR measurements, and theoretical calculations (Sec. V).

TABLE I. Characteristics of the SiC samples studied in this work.

Sample and dopant	Carrier concentration (cm^{-3})	Irradiation particle and energy	Irradiation fluence (cm^{-2})	Average positron lifetime at 300 K (ps)
1. 6*H*-SiC:Al	$p=1.6\times10^{18}$	as grown	as grown	145 ± 1
2. 6*H*-SiC:Al	$p=1.6\times10^{18}$	12 MeV protons	4×10^{15}	145 ± 1
3. 6*H*-SiC:N	$n=2.3\times10^{17}$	as grown	as grown	153 ± 1
4. 6*H*-SiC:N	$n=2.3\times10^{17}$	0.35-MeV electrons	3×10^{18}	158 ± 1
5. 6*H*-SiC:N	$n=2.3\times10^{17}$	0.8-MeV electrons	1×10^{18}	161 ± 1
6. 6*H*-SiC:N	$n=2.3\times10^{17}$	2-MeV electrons	1×10^{18}	178 ± 1
7. 6*H*-SiC:N	$n=1.9\times10^{17}$	as grown	as grown	150 ± 1
8. 6*H*-SiC:N	$n=1.9\times10^{17}$	12-MeV protons	4×10^{14}	168 ± 1
9. 6*H*-SiC:N	$n=1.9\times10^{17}$	12-MeV protons	4×10^{15}	198 ± 1
10. 6*H*-SiC:N	$n=1.9\times10^{17}$	12-MeV protons	4×10^{16}	207 ± 1
11. 6*H*-SiC:N	$n=1.9\times10^{17}$	12-MeV protons	8×10^{16}	209 ± 1

II. EXPERIMENTAL ARRANGEMENTS

A. Samples

We studied commercial (Cree Research) (0001)-oriented 6H-SiC wafers which were about 300 μm thick. Both nitrogen-doped *n*-type ($n=1.9\times10^{17}$ cm^{-3} and $n=2.3\times10^{17}$ cm^{-3}) and aluminum-doped *p*-type ($p=1.6\times10^{18}$ cm^{-3}) samples were investigated. Measurements were performed both in as-grown materials as well as after electron and proton irradiations (Table I). The production yields of different vacancy defects in the two sublattices of 6H-SiC depend on the energy of the irradiation particles incident on the sample. According to calculations of the displacement energy, 350-keV electrons are expected to damage mostly the carbon sublattice.[32] The probability of displacements in silicon sublattice should increase strongly with electron energy.[32] Here the electron energies were 0.35, 0.80, and 2.0 MeV, and the irradiation fluences were $(1-3)\times10^{18}e^-$ cm^{-2}. In proton irradiation the energy was 12 MeV, and fluences were 4×10^{14}, 4×10^{15}, 4×10^{16}, and $7.8\times10^{16}p^+$ cm^{-2}. Irradiations were done at room temperature with incident particle flux nearly parallel to the *c* axis of the SiC lattice. The protons and electrons had adequate kinetic energies to pass through the sample thickness probed by positron experiments, and variations in the defect concentration in the direction of *c* axis are thus negligible.

B. Positron experiments

Positron lifetime measurements were done using a conventional fast-fast coincidence spectrometer with a time resolution of 250 ps.[14] A 30-μ Ci ^{22}Na positron source was sandwiched between two identical sample pieces, and the positron lifetime was measured as a time interval between the two photons originating from the β^+ decay and positron annihilation. Approximately 2 million events were collected to each spectrum. The lifetime spectra

$$-\frac{dn(t)}{dt}=\sum\frac{I_i}{\tau_i}\exp(-t/\tau_i) \quad (1)$$

were analyzed as sums of exponential lifetime components τ_i weighted by the intensities I_i, convoluted with a multi-Gaussian resolution function. The average lifetime is the center of mass of the lifetime spectrum and can be calculated as $\tau_{av}=\Sigma_i I_i\tau_i$.

The positron-electron momentum distributions were measured by recording the Doppler broadening of the 511-keV annihilation radiation. A setup of two Ge detectors and a multiparameter analyzer were utilized to detect both 511-keV photons in coincidence and to reduce the background of the Doppler spectra.[33,34] An energy resolution of 0.9 keV and a peak-to-background ratio of 2×10^6 were achieved in the coincidence experiment.

Measurements were performed either in darkness or under monochromatic illumination with sub-band-gap ($h\nu=0.65-3.1$ eV) light.[29,30] The photon flux was kept constant during the measurement, but at high photon energies only a somewhat lower flux was obtained due to limitations in the intensity of the light source (halogen lamp). Photon fluxes between 10^{14} and 10^{15} cm^{-2} were used. Measurements were performed at 10–300 K and the sample temperature was varied using a closed-cycle He cryocooler.

III. IDENTIFICATION OF VACANCIES IN SiC

A. Positron lifetime results

A single lifetime component of about 145 ps can be detected in as-grown *p*-type SiC:Al samples. This lifetime has practically no temperature dependence. In good agreement with earlier results[15–20,26] or theoretical calculations,[23,35,36] we attribute the lifetime of $\tau_B=145$ ps to positrons annihilating as delocalized particles in a defect-free SiC lattice. The average positron lifetime is $\tau_{av}=153$ ps in the as-grown *n*-type SiC:N sample at room temperature. Obviously, native vacancies are present since $\tau_{av}>\tau_B$. The lifetime spectra can be decomposed to two components, the longer of which ($\tau_2=220\pm15$ ps) corresponds to positrons trapped at vacancy defects.

Electron irradiation of SiC:N samples with energies 0.35–0.8 MeV increases the average positron lifetime to about

158–161 ps after quite high irradiation fluences of $(1-3)\times10^{18}$ cm^{-2} (Table I). The lifetime spectra have a single component of about 160 ps which is constant as a function of temperature down to 10 K. Irradiations with 2-MeV energies lead to a longer average lifetime of 178 ps and increase the intensity of the 220-ps lifetime component up to 50%. When the measurement temperature is lowered to 10 K, the average lifetime decreases by more than 10 ps.

12-MeV proton irradiation of *n*-type SiC:N increases the average positron lifetime monotonically with increasing fluence (Table I). At the highest fluences of 8×10^{16} cm^{-2} saturation is seen at about $\tau_{av}=210$ ps. These lifetime spectra have only a single component which is practically independent of temperature. In proton-irradiated *p*-type SiC samples no vacancies are observed as the average positron lifetime remains at the bulk value at least up to the irradiation fluence of 4×10^{15} cm^{-2}. In these samples the irradiation-induced vacancy defects are probably in a positive charge state and thus repulsive to positrons.

The positron lifetime of about 210 ps can be attributed to a vacancy defect, which is observed in as-grown samples and produced by electron and proton irradiations. The lifetime of 160 ps dominates after electron irradiations when the irradiation energies are below 1 MeV. The average positron lifetime is constant as a function of temperature when it has been saturated to the values of $\tau_{av}=160$ or 210 ps after irradiations with large fluences. These arguments lead to the conclusion that positron lifetimes of 160 and 210 ps are associated with trapped positron states at two different vacancy defects in SiC. Obviously, the formation of 160-ps lifetime is preferred at low irradiation energies (0.35–0.8-MeV electrons) and the creation of 210-ps component dominates at high energies (2-MeV electrons, and 12-MeV protons). This suggests that the lifetimes of 160 and 210 ps correspond to vacancy defects in the C and Si sublattices, respectively. The positron lifetimes at V_C and V_{Si} simply reflect the sizes of the open volume at these vacancy defects.

Theoretical calculations give quantitative estimates for positron lifetimes at various annihilation states. According to the recent results of Staab *et al.*,[36] the calculated bulk lifetime is 131 ps, which is in reasonable agreement with the present experimental value of 145 ps. Taking into account the relaxations of atoms around vacancies,[5] a lifetime increase of $\tau_C-\tau_B=7$ ps can be expected for the C vacancy and $\tau_{Si}-\tau_B=63$ ps for the Si vacancy.[36] When scaled with our experimental value $\tau_B=145$ ps, the theory thus predicts positron lifetimes of $\tau_C=152$ ps and $\tau_{Si}=208$ ps for V_C and V_{Si} respectively. These are very close to the experimental values of 160 and 210 ps. thus supporting strongly the identification of C and Si vacancies. Furthermore, the calculation predicts that the positron lifetime at V_CV_{Si} divacancies is about 228 ps which is clearly larger than expected for V_{Si} or seen in the experiments after irradiation. In as-grown samples, however, the accuracy of the experimental lifetime of 220 ± 15 ps does not allow to distinguish between V_{Si} and $V_{Si}V_C$.

B. Electron momentum distributions of vacancy defects

The coincidence detection of the Doppler broadening spectrum yields the momentum distribution of annihilating electrons, and it is thus possible to identify the atoms surrounding the vacancy defects. We recorded the Doppler spectra at room temperature in sample numbers 5 and 11 (Table I), where practically 100% of positron annihilations takes place at vacancies corresponding to positron lifetimes of 160 and 210 ps, respectively. A minor contribution (about 5%) from the 210-ps component is seen in sample 5 according to the lifetime results. We corrected this by subtracting the spectrum recorded in sample 11, weighted with the annihilation fraction of 5%, from the data measured in sample 5.

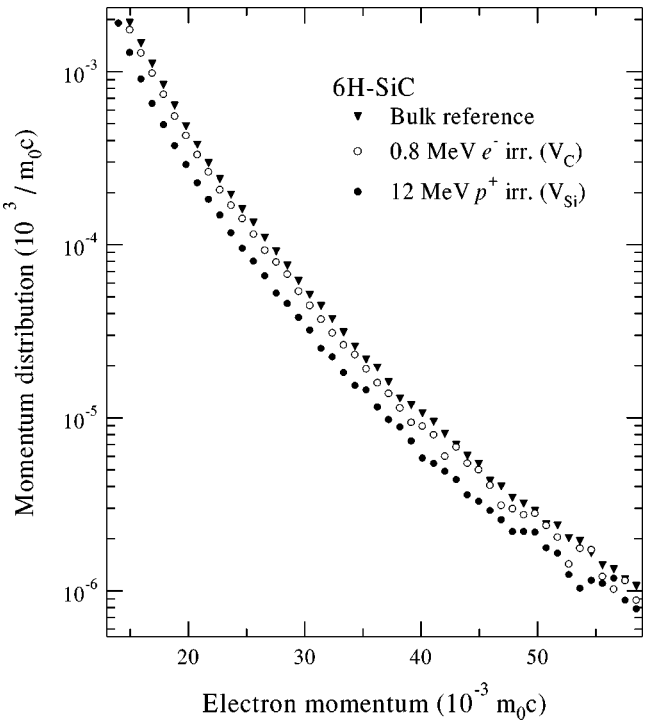

FIG. 1. Core electron momentum distributions determined by measuring the Doppler broadening of the 511-keV annihilation photons. The bulk reference was measured in defect-free Al-doped 6H-SiC (sample 1). The momentum distributions probed by positrons trapped at C and Si vacancies are recorded in 0.8-MeV electron and 12-MeV proton-irradiated SiC (samples 5 and 11, respectively).

Figure 1 shows high momentum parts of the Doppler curves for a bulk SiC lattice and for vacancies characterized by the lifetimes of 160 ps (V_C) and 210 ps (V_{Si}). In the momentum range shown annihilations take place predominantly with the outermost core electrons of Si and C (Si $2p$ and C $1s$). According to calculations,[36] the Si $2p$ electrons are clearly dominant in bulk SiC as well as at vacancies in both Si and C sublattices. The intensity of the momentum distribution in Fig. 1 thus quantifies the presence of Si $2p$ electrons in the measured system. In the bulk SiC lattice and in the vacancy with a positron lifetime of 160 ps the intensity is high, indicating a strong contribution from Si $2p$ electrons. A much lower intensity is recorded for the vacancy where the lifetime is 210 ps. Since C vacancies are surrounded by Si atoms, the results directly point toward the interpretation that 160 ps and 210-ps lifetime components arise from C and Si vacancies, respectively.

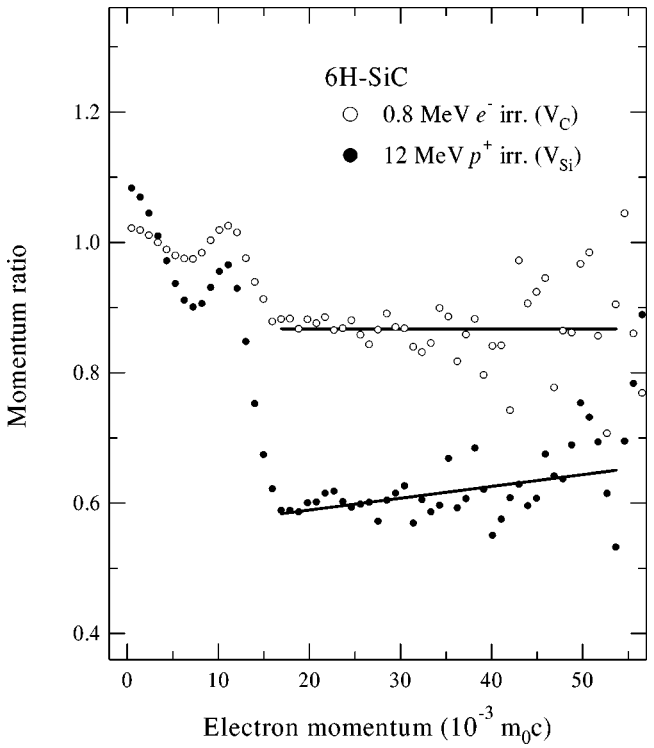

FIG. 2. The ratio of electron momentum distributions at vacancy defects and in the bulk SiC lattice. The ratio curves for 0.8-MeV electron and 12-MeV proton-irradiated SiC samples (numbers 5 and 11) characterize C and Si vacancies, respectively. The solid lines are linear fits to the momentum ratios at $(17-55)\times10^{-3}\ m_0c$.

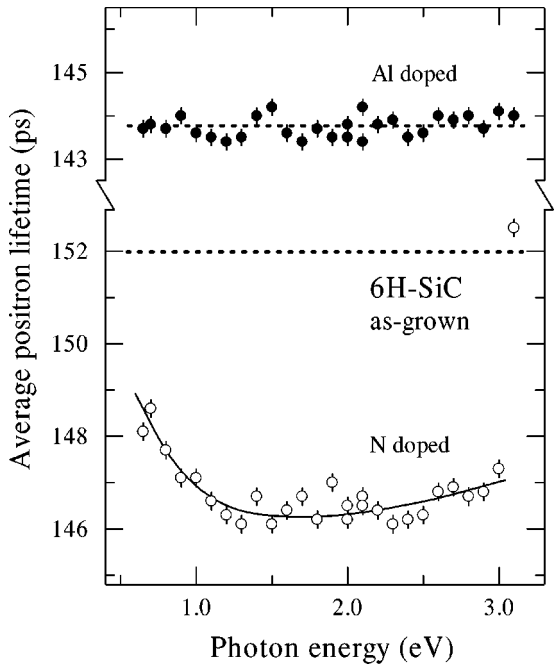

FIG. 3. Average positron lifetime in as-grown N- and Al-doped SiC, recorded at 10 K under illumination with indicated photon energies. The average positron lifetime in darkness at 10 K is shown by the dashed line. The solid line is drawn to guide the eye.

To emphasize the differences in the electron momentum distributions, Fig. 2 shows the Doppler broadening data of Si and C vacancies as momentum ratios scaled to bulk SiC. The missing Si $2p$ electrons around the Si vacancy lead to the low intensity ratio at $(15-50)\times10^{-3}m_0c$ in Fig. 2. The curves are in good agreement with the calculated ones[36] for both V_C and V_{Si}, thus supporting the identification of the defects. In fact, the momentum ratio for V_{Si} shows a small slope of $1.8\pm0.6\ m_0c^{-1}$ at the momenta of $(15-50)\times10^{-3}m_0c$ (a line fit is shown in Fig. 2). This slope can be attributed to the high-momentum of $1s$ electrons of the C atoms surrounding the Si vacancy, and a theoretical calculation predicts that such a slope should indeed be about $2(m_0c)^{-1}$.[36] On the other hand, the momentum ratio for the C vacancy is flat in this range, since Si $2p$ electrons dominate the positron annihilations both in the bulk lattice and at the C vacancy, making the ratio independent of momentum.

The momentum distribution of the Si vacancy in Fig. 2 is qualitatively similar to that published very recently by Kawasuso *et al.*[20] Compared with their work, however, here we utilize more extensively positron lifetime experiments, which show 100% positron trapping and annihilation at Si vacancy after proton irradiation with high fluence ($\geqslant4\times10^{16}$ cm^{-3}). The lifetime at V_{Si} is thus 210 ps, which is in agreement with that reported by Müller *et al.*[27] but slightly larger than the value of Kawasuso *et al.*[20] The ratio curve of Kawasuso *et al.* has a larger intensity than ours at the momenta above $20\times10^{-3}m_0c$ in Fig. 2. Also the slope in their data above $20\times10^{-3}m_0c$ is larger, although the comparison is difficult due to the relatively large statistical error of Kawasuso *et al.*[20] In general, our momentum ratio for the Si vacancy (Fig. 2) is in much better agreement with the results of theoretical calculations.[36]

The positron lifetime and Doppler broadening data thus show unambiguously that the lifetime components of 160 and 210 ps arise from annihilations at C and Si vacancies, respectively. The present data do not allow one to distinguish between isolated monovacancies and vacancy complexes. In irradiated samples, however, we think that isolated V_{Si} and V_C are the most likely candidates, for the following reasons: (i) these defects have been identified as stable ones at room temperature,[6–12] (ii) their formation is roughly linear as a function of irradiation fluence,[37] and (iii) a quantitative analysis of positron data yields high introduction rates of >0.5 cm^{-1} for V_C and V_{Si} in 2-MeV electron irradiation,[37] which is typical for simple, primary defects. On the other hand, the native Si vacancies found in as-grown *n*-type SiC (sample 3 in Table I) probably belong to defect complexes. Si vacancies are likely to be mobile at the high growth temperature of SiC, and thus stabilized only as parts of complexes, for example, with N impurity atoms.

IV. PHOTOEXCITATION OF VACANCIES

A. Positron lifetimes under monochromatic illumination at low temperatures

The average positron lifetime τ_{av} as a function of the photon energy $h\nu$ in as-grown 6*H*-SiC is presented in Fig. 3. The experiment was performed at 10 K. The average positron lifetime in darkness is shown by the dashed line. In *n*-type

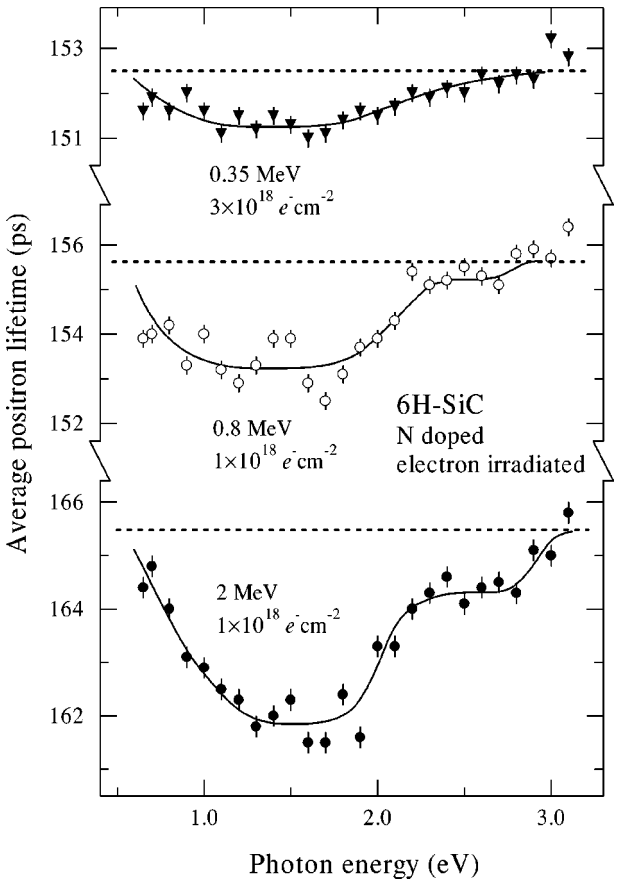

FIG. 4. Average positron lifetime in N-doped electron-irradiated SiC, recorded at 10 K under illumination with indicated photon energies. The average positron lifetime in darkness at 10 K is shown by the dashed line. The irradiation energies and fluences are given for each sample. The solid lines are drawn to guide the eye.

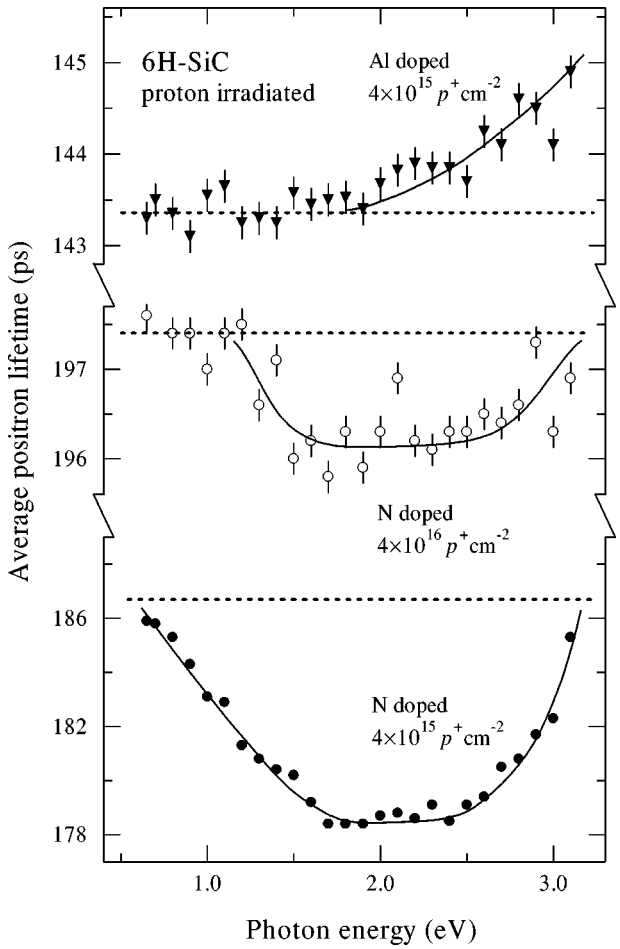

FIG. 5. Average positron lifetime in N-and Al-doped proton-irradiated SiC, recorded at 10 K under illumination with indicated photon energies. The average positron lifetime in darkness at 10 K is shown by the dashed line. The 12-MeV proton fluences are given for each sample. The solid lines are drawn to guide the eye.

SiC the illumination is found to decrease τ_{av} at all photon energies, but the effect is strongest at $h\nu > 1.0$ eV. The second lifetime component τ_2 is the same under illumination and in darkness, but the intensities of the components vary with $h\nu$. In *p*-type as-grown samples the illumination has no influence on τ_{av}.

In electron-irradiated SiC the average lifetime decreases as a function of photon energy at $h\nu < 1.5$ eV (Fig. 4) but the longer component τ_2 remains constant. Unlike in as-grown *n*-type SiC, a clear increase toward the value of τ_{av} in darkness is observed in electron-irradiated samples at photon energies above $h\nu = 2.0 \pm 0.1$ eV. Generally illumination has a stronger influence on positron lifetime in the samples irradiated with 2-MeV electrons, whereas those irradiated with 0.35–0.8-MeV energies show less sensitivity to photons. This suggests that the illumination effects are related to defects in the Si sublattice.

The average positron lifetime measured under illumination of proton-irradiated samples is shown in Fig. 5. For *n*-type samples the behavior is qualitatively similar to that in as-grown or electron-irradiated samples, but differences are seen in the details of the data. For irradiation fluences below 10^{16} cm^{-2} the onset of the decrease of τ_{av} is at about 0.6 eV and at $h\nu > 2.5$ eV the average lifetime starts to increase toward its value in darkness. In the sample irradiated with a fluence of 4×10^{16} cm^{-2} the onset of the reduction of τ_{av} has been shifted to $h\nu = 1.1 \pm 0.2$ eV. In *p*-type-irradiated SiC samples the average positron lifetime increases under illumination with photon energies larger than $h\nu = 2.0 \pm 0.2$ eV.

Figure 6 shows an example of a decomposition of positron lifetime spectra measured under illumination of the N-doped sample 9, irradiated with a proton fluence of 4×10^{15} cm^{-2}. The lifetime components are $\tau_1 = 160$ ps and $\tau_2 = 210$ ps, which correspond to positrons trapped at C and Si vacancies, respectively (Sec. III). The values of the lifetime components are constant during the illumination and also the same as in darkness, as indicated by the dashed lines. The uppermost panel of Fig. 6 shows an intensity I_2 of the lifetime component τ_2, obtained from an analysis where τ_2 has been fixed to 210 ps to reduce statistical scattering. The intensity I_2 clearly decreases below its value in darkness (dashed line) under illumination. The parameters τ_1, τ_2, and I_2 also behave similarly in the other irradiated samples. The decrease of the average lifetime under illumination of the *n*-type SiC samples (Figs. 3–5) is thus caused by the decrease of the intensity I_2.

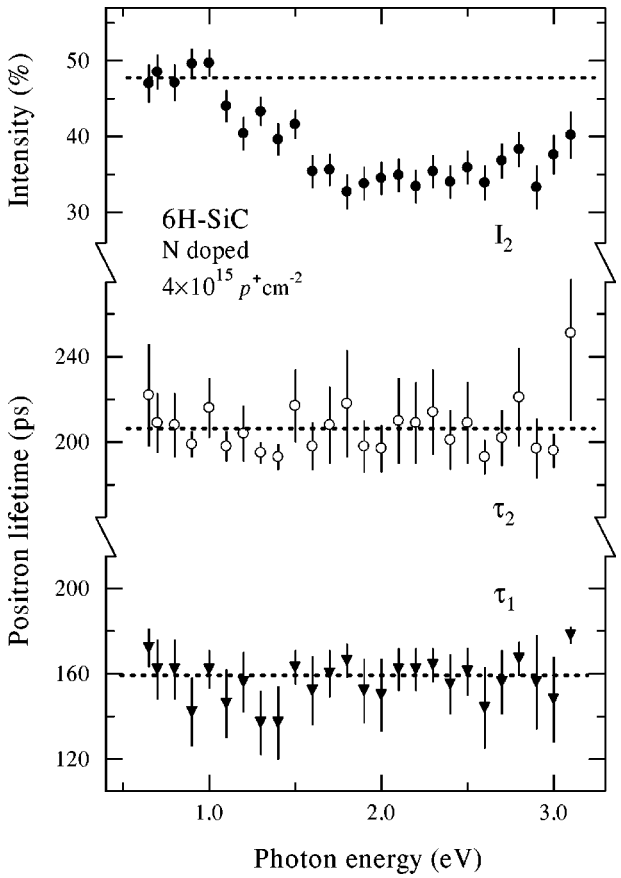

FIG. 6. The decomposed positron lifetime components τ_1 and τ_2 and intensity I_2 in N-doped SiC irradiated with a proton fluence of 4×10^{15} cm^{-2} (sample 9). The data were recorded at 10 K under illumination with indicated photon energies. The values of τ_1, τ_2, and I_2 in darkness at 10 K are shown by the dashed lines.

B. Optical transitions of the Si vacancy

The illumination-induced changes in the average positron lifetime manifest optically induced electron excitations between the conduction and valence bands and ionization levels of defects in the band gap. At low temperature, the average positron lifetime is a superposition

$$\tau_{\mathrm{av}}=\sum_i \eta_i\tau_i=\eta_B\tau_B+\eta_I\tau_I+\eta_{\mathrm{C}}\tau_{\mathrm{C}}+\tau_{\mathrm{Si}}\tau_{\mathrm{Si}}, \qquad (2)$$

where η and τ correspond to the fractions of positron annihilations and the positron lifetimes in the bulk lattice ($\eta_B,\tau_B=145$ ps), at negative ions ($\eta_I,\tau_I=145$ ps), at C vacancies ($\eta_{\mathrm{C}},\tau_{\mathrm{C}}=160$ ps) and at Si vacancies ($\eta_{\mathrm{Si}},\tau_{\mathrm{Si}}=210$ ps). The fractions of positron annihilations η_i,

$$\eta_i=\frac{\kappa_i}{\tau_B^{-1}+\Sigma_i\kappa_i}, \qquad (3)$$

depend on the positron trapping rates κ_i at V_{Si}, V_{C}, and negative ions, which are proportional to the defect concentrations c_i as

$$\kappa_i=\mu_i c_i. \qquad (4)$$

Generally, the positron trapping coefficients μ_i increase with the negative charge of the defects.[13,14] In *n*-type as-grown and irradiated SiC samples τ_{av} is smaller under illumination than in darkness. *A priori*, this could be explained either by (i) the decrease of the trapping rates at vacancy defects with a longer positron lifetime than τ_{av}, or (ii) the increase of the trapping rate at negative ions or vacancy defects which have a lifetime shorter than τ_{av}. However, we can rule out the latter possibility with the simple argumentation presented below.

In *n*-type as-grown N-doped SiC the electron levels are occupied at least up to the nitrogen ionization level at about $E_{\mathrm{C}}-0.2$ eV. The net removal rate of conduction electrons is about 20 cm^{-1} in the 12-MeV proton-irradiated samples studied here.[11] Hence at least samples 8 and 9 (Table I) remain *n*-type after proton irradiation, and their electron levels are thus filled up to the Fermi level close to $E_{\mathrm{C}}-0.2$ eV. The increase of positron trapping rate at negative ions can take place under illumination only if electrons are optically excited to their empty levels, charging them to more negative state. In the present case this is very unlikely since in *n*-type samples the levels are occupied with electrons, practically up to the conduction band.

Similarly, we can rule out illumination effects related to the carbon vacancy. Already the results in Fig. 4 suggest that illuminations have less influence on positron lifetime in samples where C vacancies are dominant. The average positron lifetime in darkness is much above the lifetime at C vacancy in proton irradiated samples 8 and 9, but a decrease in the average lifetime is observed under illumination (Fig. 5). This cannot be associated with the enhanced positron trapping due to increased negative charge of V_{C} because all electron levels are filled already in darkness almost up to the conduction band.

We thus explain the illumination effects with ionizations of electrons from the silicon vacancy. Electron excitations from V_{Si} to the conduction band decrease the negative charge of the defect, which reduces the trapping rate κ_{Si} and the annihilation fraction η_{Si} evidently leading to a lower value of the average positron lifetime under illumination than in darkness. This is directly seen in the decomposed positron lifetime data of Fig. 6, where the intensity of the $\tau_2=\tau_{\mathrm{Si}}=210$ ps lifetime component decreases under illumination. No change of the lifetime of positrons trapped at the Si vacancy is associated with the optical transitions because the lifetime component τ_2 remains constant at $\tau_2=\tau_{\mathrm{Si}}=210$ ps (Fig. 6). In samples irradiated with 0.35–0.8-MeV electrons (numbers 4 and 5) the minor illumination effects can be attributed to Si vacancies although the C vacancies are the dominant defects as explained above. In these samples the Si vacancies exist either as native defects, or they are formed in small concentrations in irradiations even with energies below 1 MeV as suggested by recent experiments.[38]

Von Bardeleben *et al.*[11] concluded that the Fermi level is pinned at the $(1-/0)$ ionization level of the Si vacancy in our proton-irradiated sample 10, since they simultaneously observed the electron paramagnetic resonances related to both $V_{\mathrm{Si}}{}^0$ and $V_{\mathrm{Si}}{}^{1-}$. In this sample, we observe a decrease of the average positron lifetime at photon energies of

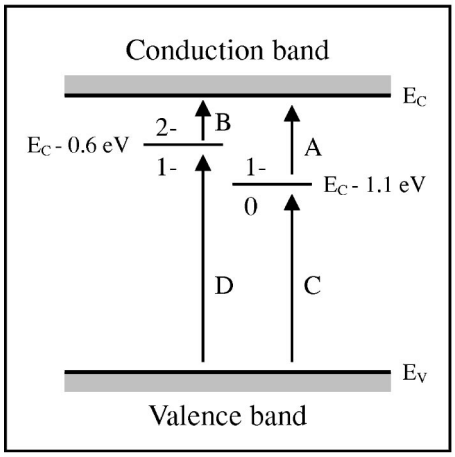

FIG. 7. Optical transitions, charge states, and estimated positions of ionization levels of the isolated Si vacancy, detected as an irradiation-induced defect in electron- and proton-irradiated SiC.

$h\nu > 1.1 \pm 0.1$ eV. We thus attribute the optical transition to the ionization of the $(1-/0)$ level of V_{Si}, i.e., transition *A* in Fig. 7. The photon energy gives an estimate of the position of the ionization level as $E_C - 1.1 \pm 0.1$ eV, where E_C is the energy of the conduction band.

In samples 3–9 the irradiation fluences are smaller than in sample 10, and thus the Fermi level is closer to the conduction band. The reduction of the average positron lifetime starts at roughly $h\nu = 0.3 \pm 0.2$ eV in as-grown samples and $h\nu = 0.6 \pm 0.1$ eV in irradiated samples. These excitations correspond to transition *B* in Fig. 7, where electrons are ionized from Si vacancies with a threshold energy of about 0.6 eV. Since the associated ionization level has higher energy and more negative charge than the $(1-/0)$ level at $E_C - 1.1$ eV, we attribute it to the (2-/1-) ionization. Its estimated position is $E_C - 0.6 \pm 0.1$ eV, but in as-grown material is seems to exist slightly closer to the conduction band at about $E_C - 0.3 \pm 0.2$ eV. The difference may reflect that isolated V_{Si} exist in irradiated samples whereas the Si vacancies in as-grown material probably belong to defect complexes.

Under illumination with photon energies $h\nu > 2.0 \pm 0.2$ eV the average positron lifetime starts to increase. In *n*-type samples it approaches the value of τ_{av} in darkness and in *p*-type SiC it clearly increases above that value. In *p*-type material most of the band gap is empty of electrons. The increase of the average positron lifetime thus indicates that electrons are optically excited from the valence band to irradiation-induced vacancies, converting them to more efficient positron traps. This filling process is obviously related to the Si vacancy, because it can surmount the ionizations of electrons from V_{Si} with transitions *A* and *B* (Fig. 7). The sum of the threshold energies of 2.0 ± 0.2 and 1.1 ± 0.2 eV (transition *A*) is equal to the energy of the 6H-SiC band gap $E_C - E_V = 3.1$ eV. We thus attribute the increase of average positron lifetime at $h\nu > 2.0 \pm 0.2$ eV to transition *C* (Fig. 7), where electrons are optically excited from the valence band to the empty $(1-/0)$ ionization level of the Si vacancy.

In the electron irradiated samples the experiments under 2.5–3.0-eV illumination yield almost the same average positron lifetime as in darkness. The illumination thus leads to the same electron occupation of the $(2-/1-)$ and $(1-/0)$ ionization levels as in darkness. This suggests that electrons are excited from the valence band to the ionization level $(2-/1-)$ with transition *D* of Fig. 7. In fact, in the data measured in samples 5 and 6 an increase of the average positron lifetime is observed to start at about $h\nu = 2.5$ eV, which correspond to the threshold energy of transition *D*.

Although the illumination effects are qualitatively similar in all *n*-type samples, the behaviors of average positron lifetime, especially the increase of τ_{av} at $h\nu > 2.0 \pm 0.2$ eV, seem to differ in details from one sample to another. This is not surprising, since efficient transitions *A* and *B* are required for filling process *C* to operate. Transitions *A* and *B*, on the other hand, compete against the thermal capture processes of photoexcited electrons. In the as-grown *n*-type sample (Fig. 3), for example, almost no evidence of the transition *C* is seen. In this sample, however, the conduction band has the largest concentration of free electrons which may overcome the optical processes *B* and *C* by becoming efficiently trapped at the ionization levels of the native Si vacancy complex.

V. CORRELATIONS TO OPTICAL AND ELECTRICAL PROPERTIES OF SiC

A. Optical absorption

The optical processes of Si vacancy in Fig. 7 are associated with absorptions of photons. The results of positron lifetime spectroscopy can thus be used to give a microscopic interpretation to more integrated quantities such as the absorption coefficient. For this purpose, simple light transmission measurements were performed in order to determine the absorption coefficient $\alpha(h\nu)$ of photons at energies below the fundamental absorption at the band edge.

The measurements were done with standard Si and Ge photodetectors in the same optical setup that was used for sample illumination in positron lifetime experiments. The absorption spectra of selected as-grown and proton irradiated samples are presented in Fig. 7. The absolute values of the absorption coefficients were not estimated but the spectra were arbitrarily scaled to $\alpha = 0$ at the lowest photon energy of $h\nu = 0.6$ eV. The data in Fig. 8 thus show the change of the absorption coefficient $\Delta\alpha(h\nu) = \alpha(h\nu) - \alpha(0.6\ \text{eV})$ from its value at $h\nu = 0.6$ eV.

In as-grown SiC:N the absorption increases smoothly with photon energy up to band-to-band absorption edge at 3.1 eV. The spectrum is qualitatively similar in as-grown samples and in proton-irradiated SiC up to the fluence of 4×10^{15} cm^{-2}. However, the slope of the α vs $h\nu$ increases with fluence demonstrating the effect of irradiation-induced defects on absorption.

The samples irradiated to proton fluences $> 10^{16}$ cm^{-2} show a clear structure in the absorption spectrum. At photon energies of $h\nu < 1$ eV the absorption increases with the irradiation fluence. This is in agreement with the positron results which show that transition *B* (Fig. 7) of the irradiation-induced Si vacancy operates at these photon energies. However, as pointed out above, the $(2-/1-)$ level of V_{Si} could

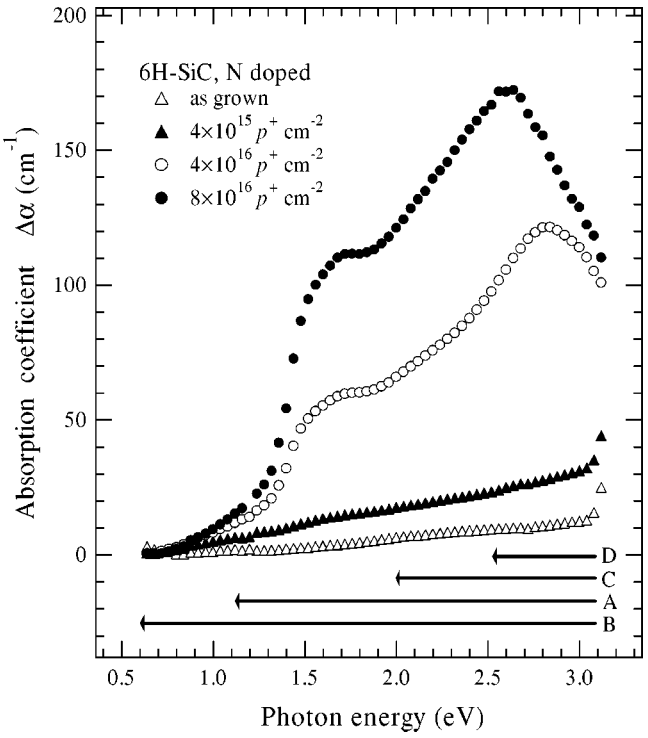

FIG. 8. Absorption spectra $\Delta\alpha(h\nu)=\alpha(h\nu)-\alpha(0.6\ \mathrm{eV})$ in N-doped as-grown and proton-irradiated SiC, recorded at 10 K. The 12-MeV proton fluences are given for each sample. The line segments $A-D$ indicate the operating range of optical transitions of Si vacancy shown in Fig. 7.

be empty of electrons after irradiations to fluences $>10^{16}\ \mathrm{cm}^{-2}$, making the absorption small.

At $h\nu>1$ eV two strong absorption edges can be seen in the spectra (Fig. 8). These edges have the typical shapes expected for optically induced transitions between deep levels and the conduction and valence bands.[39] The threshold energies for the two transitions can be estimated at $h\nu=1.1$ and 1.9 eV by fitting the energy dependent optical cross section to the data.[39] The edges of the absorption coefficient $\alpha(h\nu)$ correlate very well with those detected for Si vacancies in positron lifetime measurements. Transitions *A* and *C*, associated with the $(1-/0)$ level of V_{Si}, thus give a natural microscopic interpretation for the absorption spectrum. At photon energies $h\nu>2.5$ eV the absorption coefficient starts to decrease. At this energy range transition *D* can operate, charging more electrons to the Si vacancy. Its influence on the absorption spectrum, however, is not straightforward. The decrease of $\alpha(h\nu)$ at $h\nu>2.5$ eV can be explained by transition *A*, since the optical cross section of such a process starts to decrease at photon energies which are roughly twice the threshold energy (1.1 eV in the case of transition *A*).[39]

The absorption spectra in Fig. 8 are similar to those reported earlier after neutron irradiation.[40] Interestingly, the results of Okada *et al.*[40] showed that the absorption above 1.1 eV has the same annealing properties as the Si vacancy detected in EPR experiments. This observation is in perfect agreement with our results and the interpretations given here.

The combination of positron and absorption results allows one to estimate the optical cross sections for the ionizations of the Si vacancy. After proton irradiation fluence of $8\times10^{16}\ \mathrm{cm}^{-2}$ all positrons annihilate as trapped at V_{Si} which typically corresponds to vacancy concentrations of $[V_{\mathrm{Si}}]\approx10^{19}\ \mathrm{cm}^{-3}$.[13,14] The absorption coefficient at $h\nu=2.0$ eV is $\Delta\alpha\approx100\ \mathrm{cm}^{-1}$, which gives an estimate of $\sigma=\Delta\alpha/[V_{\mathrm{Si}}]\approx10^{-17}\ \mathrm{cm}^2$ for the optical cross section of processes *A* and *C*. This value is of the typical order of magnitude expected for optical transitions between deep levels and energy bands in semiconductors.

B. Electron paramagnetic resonance, electrical experiments, and theory

The Si vacancy has been previously identified using electron paramagnetic resonance (EPR) and its optical detection (ODMR). Von Bardeleben *et al.* recently applied EPR to study similar proton, irradiated SiC:N samples as investigated here.[11] They simultaneously detected signals from neutral and negatively charged silicon vacancies V_{Si}^0 and V_{Si}^- in samples irradiated to high proton fluences ($>10^{16}\ \mathrm{cm}^{-2}$), and concluded that the Fermi level is pinned at the $(1-/0)$ ionization level of the Si vacancy. These results are generally in good agreement with our data, as well as those published by Wimbauer *et al.*[6] and Itoh *et al.*[12]

Sörman *et al.* applied a combination of photoluminescence (PL), ODMR, and EPR to study the Si vacancy in 2.5-MeV electron irradiated 6*H*-SiC.[8] The EPR signal of a negatively charged silicon vacancy could be observed only after irradiation to a high fluence of $10^{18}\ \mathrm{cm}^{-2}$. They concluded that in as-grown samples or those irradiated to lower fluences all Si vacancies are in a doubly negative charge state. Since the EPR signal from the nitrogen donor was detected in all samples, Sörman *et al.* were able to locate the $(2-/1-)$ ionization level of V_{Si} closely below the nitrogen donor level ($E_C-0.2$ eV). This result is in good agreement with the present data, which show that the $(2-/1-)$ level of V_{Si} is about 0.6 ± 0.1 eV below the conduction band.

Sörman *et al.* further applied the ODMR to identify the neutral Si vacancy introduced in the electron irradiation.[8,9] From the energy of the PL band (1.4 eV) and its resonance excitation energy (more than 1.77 eV) they concluded that the $(0/+)$ ionization level of V_{Si} should lie at least 1.77 eV below the conduction band. Although the present experiments give no information on the $(0/+)$ level, the position estimated by Sörman *et al.* is consistent with our data. The positron experiments give evidence that the $(1-/0)$ level is at $E_C-1.1$ eV, which is thus clearly above the $(0/+)$ level as estimated by Sörman *et al.*

Deep-level transient spectroscopy (DLTS) has been applied in several publications to study native and irradiation-induced defects in SiC.[1,20,26,41–45] Various authors reported the peak labeled *R* at about $E_C-1.1$ eV in as-grown and irradiated 6*H*-SiC.[1,20,41] The *R* level has an acceptor character[1,41] and its annealing behavior is consistent with that of an isolated Si vacancy when compared with EPR or ODMR experiments.[1] Our results show that the Si vacancy has an ionization level at $E_C-1.1$ eV which is most likely associated with a transition from $1-$ to 0 charge states. We

thus conclude that the acceptor level $(1-/0)$ of V_{Si} is responsible for the *R* peak in DLTS experiments.

Several deep levels have been detected at 0.3–0.7 eV below the conduction band in DLTS measurements.[1,20,26,41,44,45] The three dominant ones are labeled E_1/E_2 at $E_C-0.34$ and $E_C-0.41$ eV, the RD_5 peak at $E_C-0.51$ eV and the Z_1/Z_2 center at $E_C-0.62$ and $E_C-0.64$ eV. The RD_5 peak has a donor character and it is probably related to the carbon vacancy.[41] The similar annealing properties of E_1/E_2 and positron annihilation data suggest that the E_1/E_2 center is associated with the Si vacancy.[20] However, E_1/E_2 seems to be slightly closer to the conduction band than estimated here for the $(2-/1-)$ transition of the irradiation-induced Si vacancy. Furthermore, the E_1/E_2 center was recently shown to have a negative-*U* character where the defect changes from negative to positive charge state when Fermi level moves below $E_C-0.41$ eV.[45] This would imply that positron trapping disappears at this center, since positrons are repulsive to positive defects. On the other hand, the Fermi level in our proton irradiated samples (fluences $>10^{16}$ cm^{-2}) is obviously below the E_1/E_2 level,[11] but yet a strong positron trapping at V_{Si} is seen. Further, the EPR data of von Bardeleben *et al.* showed that V_{Si} is either neutral or negative in these samples.[11] We thus think that it is unlikely that E_1/E_2 level is related to the isolated Si vacancy.

On the other hand, the native Si vacancy related defects in as-grown 6*H*-SiC are shown here to have ionization levels close to the conduction band at roughly $E_C-0.3(2)$ eV. This energy is in good agreement with the levels of E_1/E_2 in DLTS measurements. Furthermore, the native defects formed during growth typically have a higher thermal stability than the ones introduced by irradiation, which points the identification toward defect complexes. We thus suggest that E_1/E_2 levels in as-grown 6*H*-SiC arise from Si vacancy complexes, such as $V_{Si}-N$ pairs. During the growth these complexes may form either directly or by the migration of Si vacancy next to the N impurity.

The Z_1/Z_2 level at about $E_C-0.6$ eV is consistent with our estimate of $E_C-0.6\pm0.1$ eV for the $(2-/1-)$ ionization level of the Si vacancy. The Z_1/Z_2 center has an acceptor character[1,41] and its thermal stability is similar to that seen for the Si Vacancy in EPR or ODMR experiments.[41] We thus consider the Z_1/Z_2 level as a likely candidate for the $(2-/1-)$ ionization level of the isolated Si vacancy.

Theoretical calculations have been performed to estimate the positions of ionization levels of various point defects in SiC.[2–5] For an isolated Si vacancy in hexagonal SiC the calculations predict that $(2-/1-)$ and $(1-/0)$ ionization levels exist in the band gap.[2,5] This is in qualitative agreement with our results which indicate that these levels are at $E_C-0.6$ eV and $E_C-1.1$ eV, respectively. However, the calculated positions of the ionization levels seem to be about 1 eV lower in energy than estimated here experimentally. Obviously, the so-called Madelung correction shifts the negatively charged ionization levels closer to the measured values,[5] but a quantitative agreement between theory and experiments seems to be still lacking.

VI. CONCLUSIONS

We have applied positron annihilation spectroscopy to study vacancies in as-grown and electron- and proton-irradiated 6H-SiC. The carbon and silicon vacancies are identified as irradiation-induced defects by combining positron lifetime and two-detector Doppler broadening measurements. The experiments under monochromatic light excitation show that Si vacancies have ionization levels at $E_C-0.6$ eV and $E_C-1.1$ eV. These levels are associated with negative charge states of V_{Si} and we conclude that they correspond to $(2-/1-)$ and $(1-/0)$ ionizations of the isolated Si vacancy. In as-grown material a similar ionization level is observed slightly closer to the conduction band at roughly $E_C-0.3$ eV. We attribute it to a defect complex involving a Si vacancy.

We correlate the positron results with data obtained by optical, electrical, and spin-resonance techniques. Optical-absorption spectra show clear structures which can be attributed to transitions of electrons between the ionization levels of V_{Si} and conduction and valence bands. We suggest further that the acceptor levels observed in deep-level transient spectroscopy at $E_C-1.1$ eV the (*R* level) and $E_C-0.6$ eV (the Z_1/Z_2 level) correspond to $(2-/1-)$ and $(1-/0)$ ionizations of the Si vacancy, respectively. Finally, our results are in good agreement, and in many ways complementary, to those published earlier using electron paramagnetic resonance or its optical detection (ODMR).

[1] T. Dalibor, G. Pensl, H. Matsunami, T. Kimoto, W. J. Choyke, A. Schöner, and N. Nordell, Phys. Status Solidi A **162**, 199 (1997).
[2] A. Zywietz, J. Furthmüller, and F. Bechstedt, Phys. Rev. B **59**, 15 166 (1999).
[3] A. Zywietz, J. Furthmüller, and F. Bechstedt, Phys. Rev. B **62**, 6854 (2000).
[4] L. Torpo, R. M. Nieminen, K. E. Laasonen, and S. Pöykkö, Appl. Phys. Lett. **74**, 221 (1999).
[5] L. Torpo, M. Marlo, T. E. M. Staab, and R. M. Nieminen, J. Phys.: Condens. Matter **13**, 6203 (2001).
[6] T. Wimbauer, B. K. Meyer, A. Hofstaetter, A. Scharmann, and H. Overhof, Phys. Rev. B **56**, 7384 (1997).
[7] N. T. Son, E. Sörman, W. M. Chen, O. Kordina, B. Monemar, and E. Janzen, Appl. Phys. Lett. **65**, 2687 (1994).
[8] E. Sörman, N. T. Son, W. M. Chen, O. Kordina, C. Hallin, and E. Janzen, Phys. Rev. B **61**, 2613 (2000).
[9] M. Wagner, B. Magnusson, W. M. Chen, E. Janzen, E. Sörman, C. Hallin, and J. L. Lindström, Phys. Rev. B **62**, 16 555 (2000).
[10] H. J. von Bardeleben, J. L. Cantin, L. Henry, and M. F. Barthe, Phys. Rev. B **62**, 10 841 (2000).
[11] H. J. von Bardeleben, J. L. Cantin, I. Vickridge, and G. Battistig, Phys. Rev. B **62**, 10 126 (2000).
[12] H. Itoh, A. Kawasuso, T. Ohshima, M. Yoshikawa, I. Nashiyama, S. Tanigawa, S. Misawa, H. Okumura, and S. Yoshida, Phys. Status Solidi A **162**, 173 (1997).
[13] K. Saarinen, P. Hautojärvi, and C. Corbel, in *Identification of*

Defects in Semiconductors, edited by M. Stavola (Academic, New York, 1998), p. 209.
[14] R. Krause-Rehberg and H. S. Leipner, *Positron Annihilation in Semiconductors* (Springer, Heidelberg, 1999).
[15] C. C. Ling, C. D. Beling, and S. Fung, Phys. Rev. B **62**, 8016 (2000).
[16] A. Polity, S. Huth, and M. Lausmann, Phys. Rev. B **59**, 10 603 (1999).
[17] A. Kawasuso, H. Itoh, S. Okada, and H. Okumura, J. Appl. Phys. **80**, 5639 (1996).
[18] A. Kawasuso, H. Itoh, T. Ohshima, K. Abe, and S. Okada, J. Appl. Phys. **82**, 3232 (1996).
[19] A. Kawasuso, R. Redmann, R. Krause-Rehberg, M. Yoshikawa, K. Kojima, and H. Itoh, Phys. Status. Solidi B **223**, R8 (2001).
[20] A. Kawasuso, R. Redmann, R. Krause-Rehberg, T. Frank, M. Weidner, G. Pensl, P. Sperr, and H. Itoh, J. Appl. Phys. **90**, 3377 (2001).
[21] W. Puff, A. G. Balogh, and P. Mascher, in *Microstructural Processes in Infrared Materials*, edited by S. J. Zinkle, G. Lucas, R. Ewing, and J. Williams, MRS Symposia Proceedings No. 540 (Materials Research Society, Pittsburgh, 1999), p. 177.
[22] W. Puff, A. G. Balogh, and P. Mascher, Mater. Sci. Forum **338–342**, 969 (2000).
[23] G. Brauer, W. Anwand, P. G. Coleman, A. P. Knights, F. Plazaola, Y. Pacaud, W. Skorupa, J. Störmer, and P. Willutzki, Phys. Rev. B **54**, 3084 (1996).
[24] M.-F. Barthe, L. Henry, C. Corbel, G. Blondiaux, K. Saarinen, P. Hautojärvi, E. Hugonnard, L. Di Cioccio, F. Letertre, and B. Ghyselen, Phys. Rev. B **62**, 16 638 (2000).
[25] D. T. Britton, M.-F. Barthe, C. Corbel, A. Hempel, L. Henry, P. Desgardin, W. Bauer-Kugelmann, G. Kögel, P. Sperr, and W. Triftshäuser, Appl. Phys. Lett. **78**, 1234 (2001).
[26] M. Gong, S. Fung, C. D. Beling, and Z. You, J. Appl. Phys. **85**, 7604 (1999).
[27] M. A. Müller, A. A. Rempel, K. Reichle, W. Sprengel, J. Major, and H.-E. Schaefer, Mater. Sci. Forum **363–365**, 70 (2001).
[28] F. Redmann, A. Kawasuso, K. Petters, R. Krause-Rehberg, and H. Itoh, Mater. Sci. Forum **363–365**, 126 (2001).
[29] K. Saarinen, S. Kuisma, P. Hautojärvi, C. Corbel, and C. LeBerre, Phys. Rev. Lett. **70**, 2794 (1993).
[30] S. Kuisma, K. Saarinen, P. Hautojärvi, C. Corbel, and C. LeBerre, Phys. Rev. B **53**, 9814 (1996).
[31] H. Kauppinen, C. Corbel, J. Nissilä, K. Saarinen, and P. Hautojärvi, Phys. Rev. B **57**, 12 911 (1998).
[32] H. Inui, H. Mori, and H. Fujita, Philos. Mag. B **61**, 107 (1990).
[33] M. Alatalo, H. Kauppinen, K. Saarinen, M. J. Puska, J. Mäkinen, P. Hautojärvi, and R. M. Nieminen, Phys. Rev. B **51**, 4176 (1995).
[34] P. Asoka-Kumar, M. Alatalo, V. J. Ghosh, A. C. Kruseman, B. Nielsen, and K. G. Lynn, Phys. Rev. Lett. **77**, 2097 (1996).
[35] G. Brauer, W. Anwand, E.-M. Nicht, J. Kuriplach, M. Sob, N. Wagner, P. G. Coleman, M. J. Puska, and T. Korhonen, Phys. Rev. B **54**, 2512 (1996).
[36] T. Staab, L. M. Torpo, M. J. Puska, and R. M. Nieminen, Mater. Sci. Forum **353–356**, 533 (2001).
[37] More details concerning the introduction of vacancies and negative ions in irradiated 6*H*-SiC will be published separately.
[38] J. W. Steeds, F. Carosella, G. A. Evans, M. M. Ismail, L. R. Danks, and W. Voegeli, Mater. Sci. Forum **353–356**, 381 (2001).
[39] A. Chantre, G. Vincent, and D. Bois, Phys. Rev. B **23**, 5335 (1981).
[40] M. Okada, K. Atobe, M. Nakagawa, S. Kanazawa, I. Kanno, and I. Kimura, Nucl. Instrum. Methods Phys. Res. B **166–167**, 399 (2000).
[41] M. O. Aboelfotoh and J. P. Doyle, Phys. Rev. B **59**, 10823 (1999).
[42] C. Hemmingsson, N. T. Son, O. Kordina, J. P. Bergman, E. Janzen, J. L. Lindström, S. Savage, and N. Nordell, J. Appl. Phys. **81**, 6155 (1997).
[43] C. G. Hemmingsson, N. T. Son, A. Ellison, J. Zhang, and E. Janzen, Phys. Rev. B **58**, 10 119 (1998).
[44] C. Hemmingsson, N. T. Son, O. Kordina, E. Janzen, and J. L. Lindström, J. Appl. Phys. **84**, 704 (1998).
[45] C. G. Hemmingsson, N. T. Son, and E. Janzen, Appl. Phys. Lett. **74**, 839 (1999).